#### GEOPHYSICAL RESEARCH LETTERS

Supporting Information for "Water vapor spectroscopy and thermodynamics constrain Earth's tropopause temperature"

Brett A. McKim<sup>1</sup>, Nadir Jeevanjee<sup>2</sup>, Geoffrey K. Vallis<sup>1</sup>, Neil Lewis<sup>1</sup>

<sup>1</sup>University of Exeter, Stocker Rd, EX4 4PY Exeter, UK

 $^2{\mbox{Geophysical Fluid Dynamics Laboratory, Princeton, NJ, USA}$ 

# **Additional Figures**

### Discussion of stratospheric water vapor

We check the importance of stratospheric water vapor by examining the sensitivity of  $f_{\kappa}(p)$  to perturbations in stratospheric humidity. We take the single column model control simulation (which does not include ozone) and then perturb the amount of stratospheric water vapor that is passed to the offline line-by-line radiation scheme used to calculate quantities such as spectrally resolved optical depth and radiative cooling. This allows us to isolate the effect of increased stratospheric water vapor, and when we reach an Earth-like value of stratospheric humidity of 3 to 4 ppmv, we can test whether the arguments used to constrain the tropopause temperature have changed qualitatively from the control simulation.

The chosen values of the stratospheric water vapor to be passed to the line-by-line radiation scheme are plotted in the top row of Figure S9. First, there is the control run in gray (which results from our imposed constraint that stratospheric humidity should not increase with height), and then a few curves in blue corresponding to a constant stratospheric vapor mass mixing ratio value of  $1 \times 10^{-7}$  kg/kg,  $1 \times 10^{-6}$  kg/kg, and  $2 \times 10^{-6}$  kg/kg. The last one most closely resembles the observed value of stratospheric humidity of 3 to 4 ppmy (see Figure 8a of Fueglistaler et al. (2009).

We can check whether the argument that leads to our constraint on the tropopause temperature is qualitatively different for a stratosphere with an Earth-like value of moisture. Recall that our heuristic argument starts from Equation 6 of the main text, where we see that there is a proportionality between the radiative cooling at a given height  $Q_{\text{CTS}}(p)$  and the density of wavenumbers emitting to space at a given height  $f_{\kappa}(p)$ . The constraint we propose for the radiative tropopause is that where  $f_{\kappa}(p) \to 0$  corresponds to where  $Q_{\text{CTS}}(p) \to 0$  (and also the total radiative cooling Q). To be more precise, it is where  $f_{\kappa}(p) \to 0$  first becomes much smaller than its upper tropospheric value; and the same for Q. Our theory should be valid if this condition is satisfied. Let us examine  $f_{\kappa}(p)$  in these simulations.

We plot  $f_{\kappa}(p)$  for the different simulations in the second row of Figure S9 and record the value of  $f_{\kappa}$  at the tropopause  $f_{tp}$  (diagnosed by the radiative cooling criterion), its max value in the upper troposphere  $f_{max}$  and the ratio between the two. This number should be small with respect to 1 for our arguments to hold. When we plot  $f_{\kappa}(p)$  for the control simulation, and for a constant stratospheric humidity value of  $10^{-7}$  kg/kg,  $10^{-6}$ 

kg/kg, and the Earth-like value of  $2 \times 10^{-6}$  kg/kg, we see the condition is satisfied, as

 $f_{tp}$  is about one to two orders of magnitude less than  $f_{max}$  in all cases, consistent with

the decline in radiative cooling between the upper troposphere and at the tropopause.

There are some quantitative differences between simulations, but not qualitative ones.

Thus, our argument that leads to a constraint on tropopause temperature is robust to

reasonable perturbations in stratospheric humidity. This is also supported by the small

stratospheric contribution to water vapor optical depth and longwave radiative cooling at

the tropopause (plotted in the third and fourth row of Figure S9).

To a good approximation, we can therefore ignore the stratospheric contribution to

water vapor optical depth and longwave radiative cooling to space when deriving our

expression for tropopause temperature, at the expense of a small numerical error.

At the same time, the net effect of stratospheric water vapor on the OLR is to reduce

it by about 1 Wm<sup>-2</sup> between the driest and wettest simulations, which is consistent with

other work showing the importance of water vapor in modulating the Earth's greenhouse

effect (Solomon et al., 2010; Dessler et al., 2013).

Methods

Isca Framework

For all simulations, we use Isca, a modeling framework that makes it easy to vary

between configurations (Vallis et al., 2018). We use Isca configured as a clear-sky general

circulation model (GCM) and a clear-sky single column model (SCM). There is no sea

ice, land, or topography. The GCM and SCM configurations use the same column-wise

physics routines (e.g., radiative transfer, convective adjustment).

In the GCM, we run at T42 resolution with 40 vertical levels, distributed according to  $\sigma = \exp[-7(0.25\tilde{z} + 0.75\tilde{z}^7)]$ , where  $\tilde{z}$  is evenly spaced on the unit interval. This distribution produces levels that are roughly evenly spaced in the troposphere, and spaced more closely in the stratosphere to mitigate the increasingly coarse resolution that results from distributing levels along evenly spaced intervals of p. We use a slab mixed-layer ocean with a standard specified meridional profile of sea surface temperatures (Neale & Hoskins, 2000):

$$T_s(\phi) = \begin{cases} 300(1 - \sin^2(3\phi/2)) \text{ K,} & \text{for } -\pi/3 < \phi < \pi/3\\ 273 \text{ K,} & \text{otherwise,} \end{cases}$$
 (1)

where  $\phi$  is the latitude.

In the SCM, we run at 80 vertical levels, necessarily omit the dynamical core, and constrain stratospheric water vapor so that it cannot increase with height. We prescribe surface temperature in increments of 10 K by setting the mixed-layer temperature and then setting its depth to 10<sup>9</sup> m. Sometimes we require obtaining the height of the grid levels, in which case we numerically integrate the hypsometric equation which requires the profiles of atmospheric pressure and temperature.

In both models, we use the simple Betts-Miller convection scheme (Frierson, 2007; O'Gorman & Schneider, 2008), which drives the free troposphere to a prescribed relative humidity of 70%. Large scale condensation is included to prevent supersaturation, following (Frierson et al., 2006), and all condensed water returns immediately to the surface. Boundary layer turbulence is parameterized using a k-profile scheme similar to Troen and Mahrt (1986), and diffusion coefficients are obtained from Monin-Obukhov similarity theory (in the column model, this computation uses a prescribed surface wind

of 5 m s<sup>-1</sup>). In the SCM, we set the boundary layer depth to the lifting condensation level. For consistency, we also use this method to determine the boundary layer depth in the GCM.

In both the GCM and the SCM, we compute radiative transfer primarily with RRTM (Mlawer et al., 1997). The incoming solar radiation meridional profile resembles Earth's seasonally-averaged profile with a Second Legendre Polynomial. The surface albedo is set to 0.2. CO<sub>2</sub> and water vapor are the only greenhouse gasses (unless specified otherwise). In the SCM, we also run experiments with gray radiative transfer configured to resemble the setup of (Frierson et al., 2006), in which water vapor has no effect on radiative fluxes. That is, the gray optical depth is

$$\tau = \tau_0 \left[ f_\ell \left( \frac{p}{p_s} \right) + (1 - f_\ell) \left( \frac{p}{p_s} \right)^4 \right],\tag{2}$$

where  $\tau_0 = 6$  is the surface optical depth and  $f_{\ell} = 0.1$  is a constant. See (Frierson et al., 2006) and the Isca documentation (https://execlim.github.io/Isca/index.html) for details. Atmospheric shortwave absorption is turned off, the surface albedo is still set to 0.2 and the stellar constant is set to 342.5 Wm<sup>2</sup> unless stated otherwise.

When water vapor is coupled to the gray radiative transfer scheme, our approach resembles (Byrne & O'Gorman, 2013). That is, the optical depth is calculated as a function of specific humidity q (kg kg<sup>-1</sup>),

$$\frac{d\tau}{d\sigma} = bq,\tag{3}$$

where b = 1997.9 and  $\sigma = p/p_0$ , the pressure normalized by a constant (10<sup>5</sup> Pa). See (Byrne & O'Gorman, 2013; Vallis et al., 2018) for details.

Diagnosing the tropopause

The radiative tropopause is diagnosed as the lowest layer of atmosphere where radiative

cooling goes to zero. In the absence of radiative heating from ozone, the radiative cooling

profile asymptotes to zero in the upper troposphere and so a threshold of  $-0.05 \text{ K day}^{-1}$ 

is used for the SCM and  $-0.2 \text{ K day}^{-1}$  for the GCM. To make the diagnostic less sensitive

to model's vertical resolution, the vertical profiles of temperature, pressure, and radiative

cooling are linearly interpolated from 40 (GCM) or 80 (SCM) levels to 800.

The lapse rate tropopause is diagnosed as where the lapse rate is smaller than  $-5 \text{ K km}^1$ .

This nonstandard threshold is used because there is no ozone present in our simulations,

and because the more common choice of 2 K km<sup>-1</sup> is sensitive to Earth's present day

climate (Vallis, 2017). Again, the vertical profiles of temperature, pressure, and radiative

cooling are linearly interpolated.

Water vapor spectroscopy

We use PyRADS, a validated line-by-line column model (Koll & Cronin, 2018), to plot

the spectral line absorption coefficients of water vapor. These data are sourced from the

HITRAN 2016 database (Gordon et al., 2017), with a Lorenz line profile assumed for all

lines unless specified otherwise. Data is plotted with 0.1 cm<sup>-1</sup> spectral resolution unless

specified otherwise.

Table of constants and their values

See Table S1.

References

Byrne, M. P., & O'Gorman, P. A. (2013). Land-ocean warming contrast over a wide range of climates: Convective quasi-equilibrium theory and idealized simulations. *Journal of Climate*, 26(12), 4000 - 4016. doi: https://doi.org/10.1175/JCLI-D-12-00262.1

- Clough, S. A., Iacono, M. J., & Moncet, J.-L. (1992). Line-by-line calculations of atmospheric fluxes and cooling rates: Application to water vapor. *Journal of Geophysical Research: Atmospheres*, 97(D14), 15761-15785. doi: https://doi.org/10.1029/92JD01419
- Dessler, A. E., Schoeberl, M. R., Wang, T., Davis, S. M., & Rosenlof, K. H. (2013).

  Stratospheric water vapor feedback. *Proceedings of the National Academy of Sciences*,

  110(45), 18087-18091. doi: 10.1073/pnas.1310344110
- Frierson, D. M. W. (2007). The dynamics of idealized convection schemes and their effect on the zonally averaged tropical circulation. *Journal of the Atmospheric Sciences*, 64(6), 1959 1976. doi: https://doi.org/10.1175/JAS3935.1
- Frierson, D. M. W., Held, I. M., & Zurita-Gotor, P. (2006). A gray-radiation aquaplanet moist gcm. part i: Static stability and eddy scale. *Journal of the Atmospheric Sciences*, 63(10), 2548 2566. doi: https://doi.org/10.1175/JAS3753.1
- Fueglistaler, S., Dessler, A. E., Dunkerton, T. J., Folkins, I., Fu, Q., & Mote, P. W. (2009). Tropical tropopause layer. Reviews of Geophysics, 47(1). doi: https://doi.org/10.1029/2008RG000267
- Gordon, I., Rothman, L., Hill, C., Kochanov, R., Tan, Y., Bernath, P., ... Zak, E. (2017). The hitran 2016 molecular spectroscopic database. *Journal of Quantitative Spectroscopy and Radiative Transfer*, 203, 3-69. (HITRAN 2016 Special Issue) doi:

https://doi.org/10.1016/j.jqsrt.2017.06.038

- Jeevanjee, N., & Fueglistaler, S. (2020). Simple spectral models for atmospheric radiative cooling. *Journal of the Atmospheric Sciences*, 77(2), 479 497. doi: https://doi.org/10.1175/JAS-D-18-0347.1
- Jucker, M., & Gerber, E. P. (2017). Untangling the annual cycle of the tropical tropopause layer with an idealized moist model. *Journal of Climate*, 30(18), 7339 7358. doi: https://doi.org/10.1175/JCLI-D-17-0127.1
- Koll, D. B., & Cronin, T. W. (2018). Earth's outgoing longwave radiation linear due to h2o greenhouse effect. Proceedings of the National Academy of Sciences, 115(41), 10293-10298. doi: 10.1073/pnas.1809868115
- Mlawer, E. J., Taubman, S. J., Brown, P. D., Iacono, M. J., & Clough, S. A. (1997).
  Radiative transfer for inhomogeneous atmospheres: Rrtm, a validated correlated-k
  model for the longwave. Journal of Geophysical Research: Atmospheres, 102(D14),
  16663-16682. doi: https://doi.org/10.1029/97JD00237
- Neale, R. B., & Hoskins, B. J. (2000). A standard test for agems including their physical parametrizations: I: the proposal. *Atmospheric Science Letters*, 1(2), 101-107. doi: https://doi.org/10.1006/asle.2000.0022
- O'Gorman, P. A., & Schneider, T. (2008). The Hydrological Cycle over a Wide Range of Climates Simulated with an Idealized GCM. *Journal of Climate*, 21(15), 3815. doi: 10.1175/2007JCLI2065.1
- Solomon, S., Rosenlof, K. H., Portmann, R. W., Daniel, J. S., Davis, S. M., Sanford, T. J., & Plattner, G.-K. (2010). Contributions of stratospheric water vapor to

decadal changes in the rate of global warming. Science, 327(5970), 1219-1223. doi: 10.1126/science.1182488

- Troen, I. B., & Mahrt, L. (1986, October). A simple model of the atmospheric boundary layer; sensitivity to surface evaporation. *Boundary-Layer Meteorology*, 37(1-2), 129-148. doi: 10.1007/BF00122760
- Vallis, G. K. (2017). Atmospheric and oceanic fluid dynamics: Fundamentals and large-scale circulation (2nd ed.). Cambridge University Press. doi: 10.1017/9781107588417
- Vallis, G. K., Colyer, G., Geen, R., Gerber, E., Jucker, M., Maher, P., . . . Thomson, S. I. (2018). Isca, v1.0: a framework for the global modelling of the atmospheres of earth and other planets at varying levels of complexity. Geoscientific Model Development, 11(3), 843–859. doi: 10.5194/gmd-11-843-2018

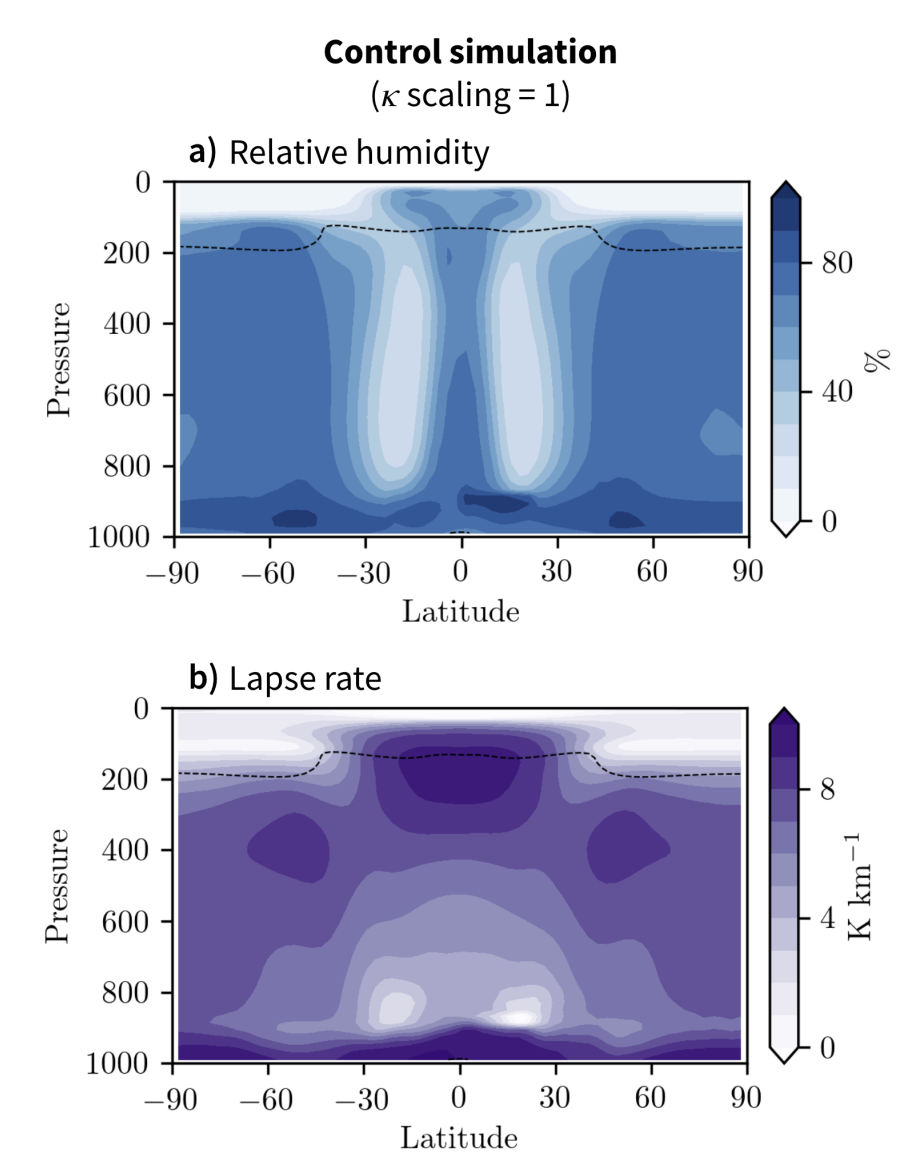


Figure S1. Zonal-mean profiles from control Isca aquaplanet simulation. (a) Relative humidity. (b) Lapse rate. The dashed line indicates the radiative tropopause using the  $-0.2 \text{ K day}^{-1}$  criterion. The globally averaged tropospheric lapse rate is 7 K km<sup>-1</sup>, defined here as the region between the average lifting condensation level ( $\approx 950 \text{ hPa}$ ) and the average tropopause height ( $\approx 150 \text{ hPa}$ ).

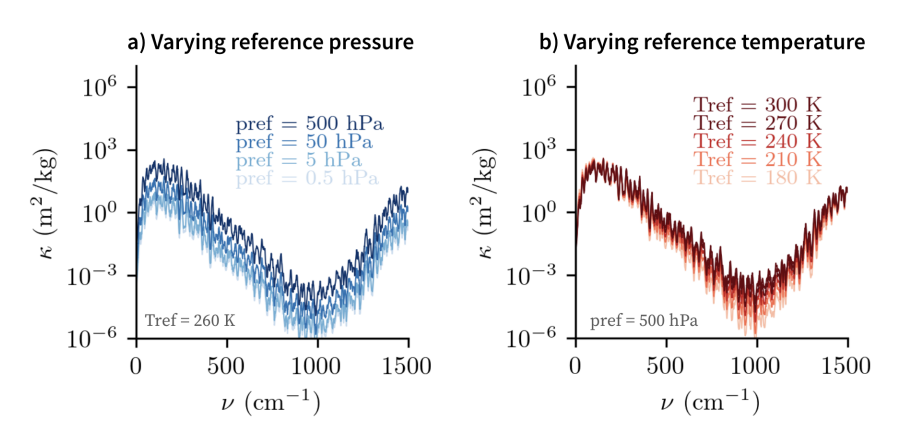


Figure S2. Effect of varying reference pressure and temperature on water vapor absorption coefficients. (a) Varying reference pressure while holding reference temperature (260 K) fixed. (b) Varying reference temperature while holding reference pressure (500 hPa) fixed.

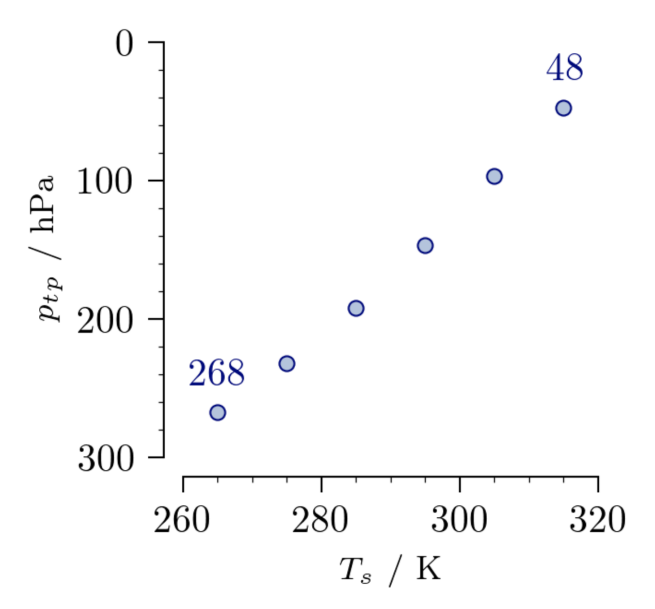


Figure S3. Effect of surface temperature on tropopasue pressure in the ISCA single column model. Tropopause pressure varies by a factor of five between the coldest and warmest simulations, whereas tropopause temperature varies by less than 10% (Figure 2c).

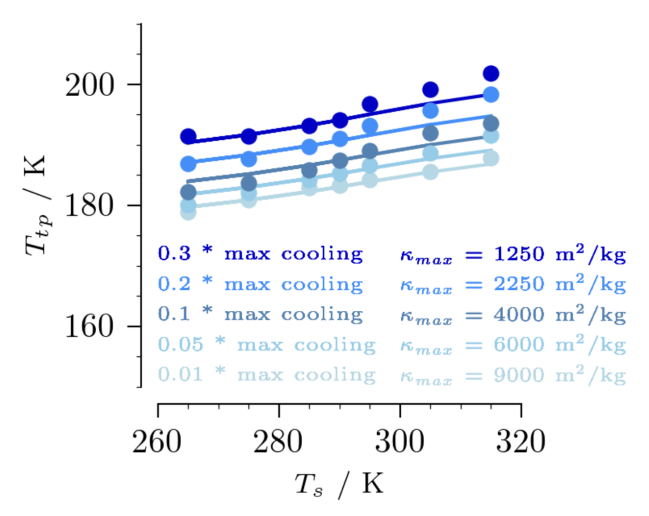


Figure S4. Effect of varying the radiative cooling criterion used to diagnose the radiative tropopause. Dots indicate tropopause temperature of the Isca single column model; lines indicate the tropopause temperature predicted from the thermospectric constraint. The threshold used is a coefficient multiplied by the maximum value of radiative cooling in the column. The tuned value of  $\kappa_{\text{max}}$  in the thermospectric constraint is displayed.

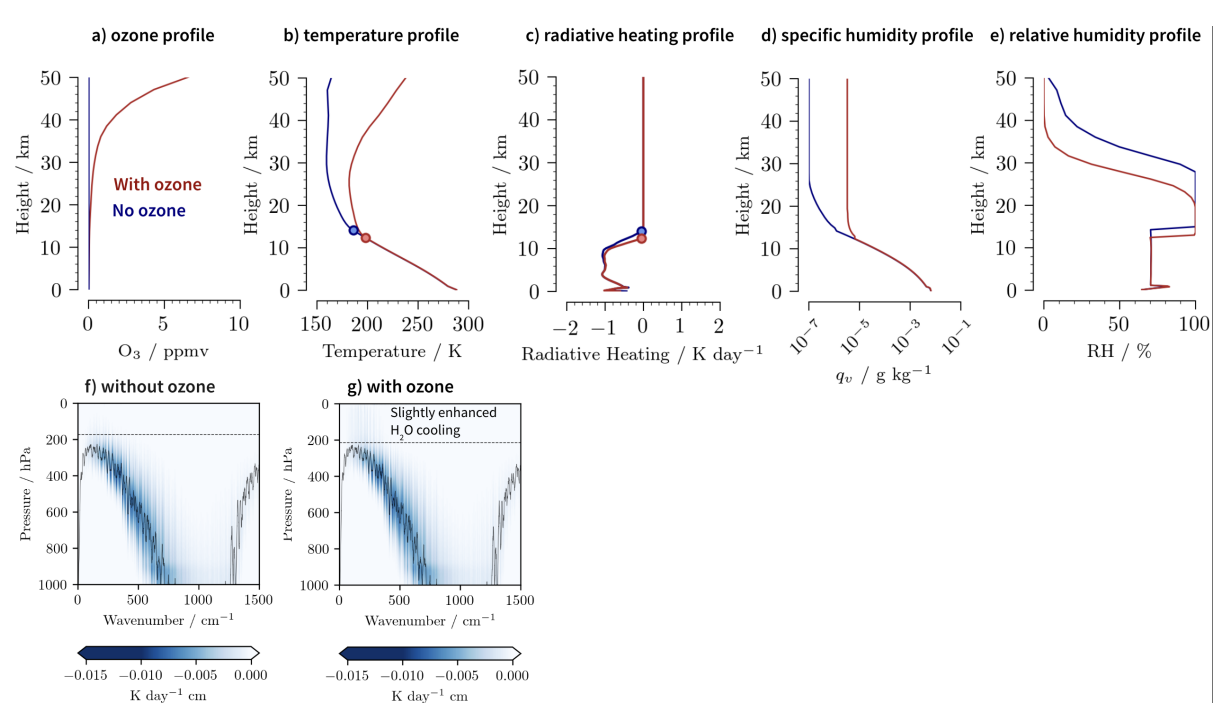


Figure S5. Effect of ozone and enhanced stratospheric moisture on the atmosphere.

(a) A typical ozone profile is used (Vallis et al., 2018; Jucker & Gerber, 2017). (b) The temperature profile. Dots indicate the radiative tropopause. (c) The net radiative cooling profile from all species. (d) The profile of specific humidity. (f,g) Spectrally-resolved longwave radiative cooling to space from water vapor only, computed with PyRADS.

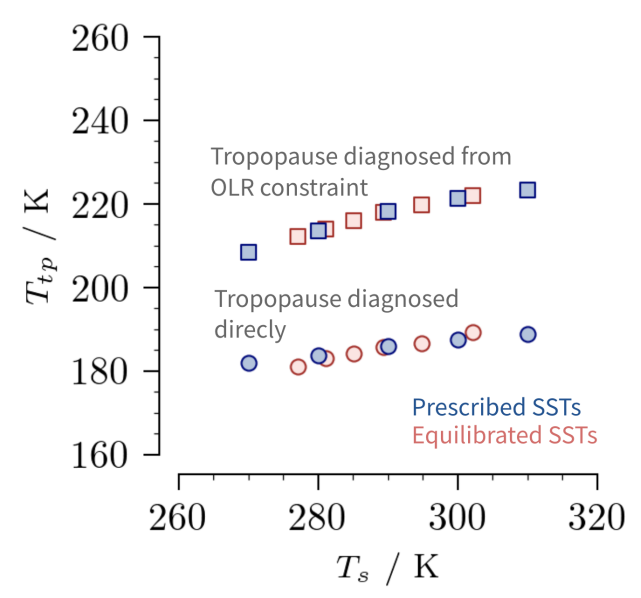


Figure S6. The effect of using equilibrated SSTs vs prescribed SSTs. In red, the experiment using changes in insolation in equal increments between 91% and 106% of the present day value to increase surface temperature in a way such that TOA energy balance is maintained (red dots and squares). In blue, the experiment using changes in the prescribed SST to inscrease surface temperature. This method causes a difference between the incoming solar and outgoing longwave radiation. The latter method is used in the main text.

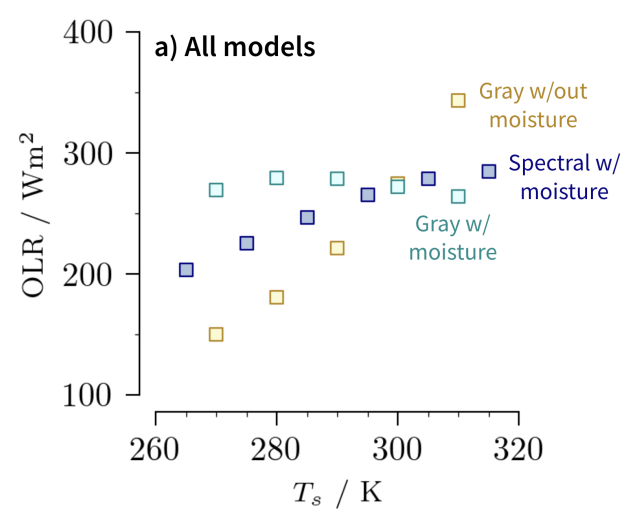
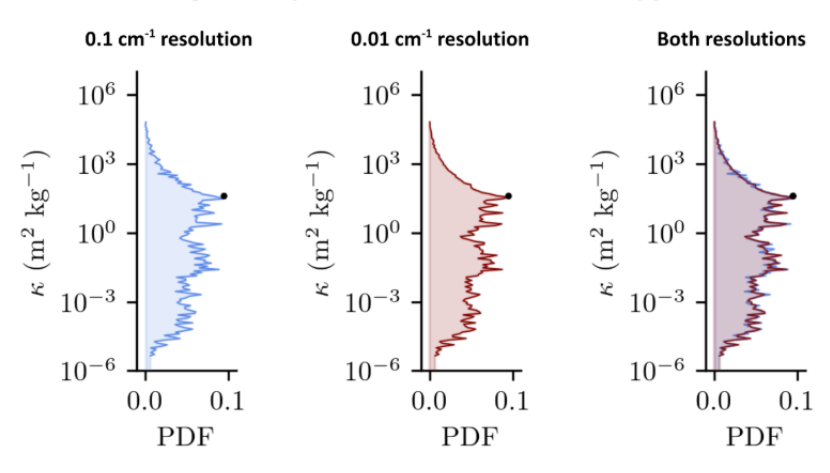


Figure S7. Dependence of Outgoing Longwave Radiation (OLR) on surface temperature. Surface temperature is varied in the ISCA single column model from 265 K to 310 K for climate models with dry gray, moist gray, and spectral radiative transfer. (a) Outgoing longwave radiation (OLR) from the climate models configured with different radiative transfer.

## Testing the impact of resolution on the kappa distribution



### Testing the impact of lineshapes on the radiative cooling profile

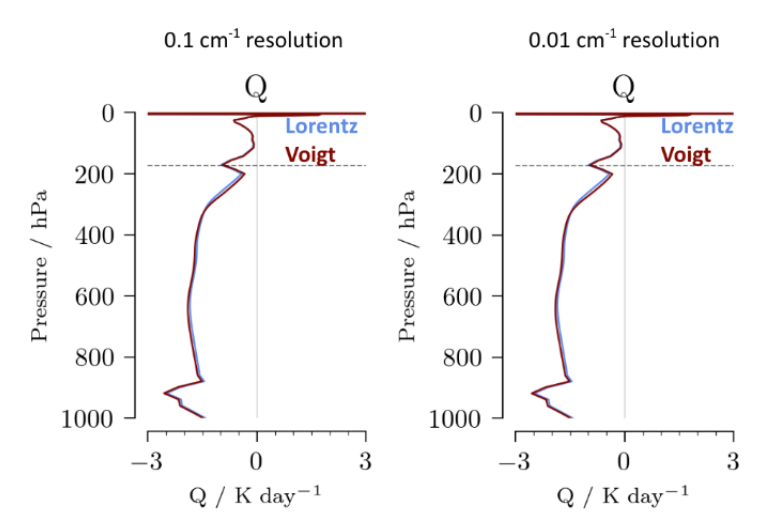


Figure S8.  $\kappa_{H_2O}$  distribution and radiative cooling profile insensitive to spectral resolution and line shape assumptions. (top) Using the PyRADS offline spectral radiative transfer code with the default Isca SCM simulation, the spectral resolution is increased from the default of 0.1 cm<sup>-1</sup> to 0.01 cm<sup>-1</sup>. (bottom) The line shape assumption is varied from the default of Lorentz to Voigt. This is done for a spectral resolution of 0.1 and 0.01 cm<sup>-1</sup>.

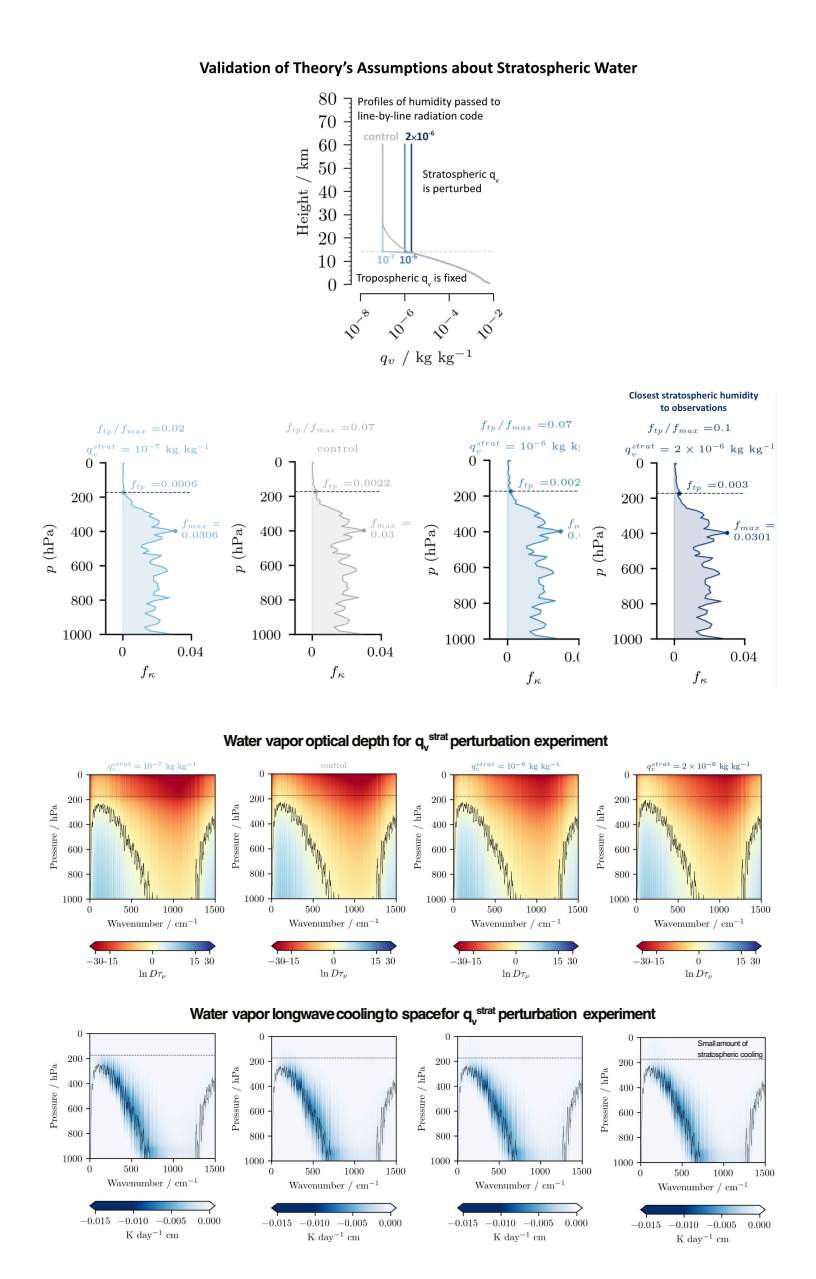
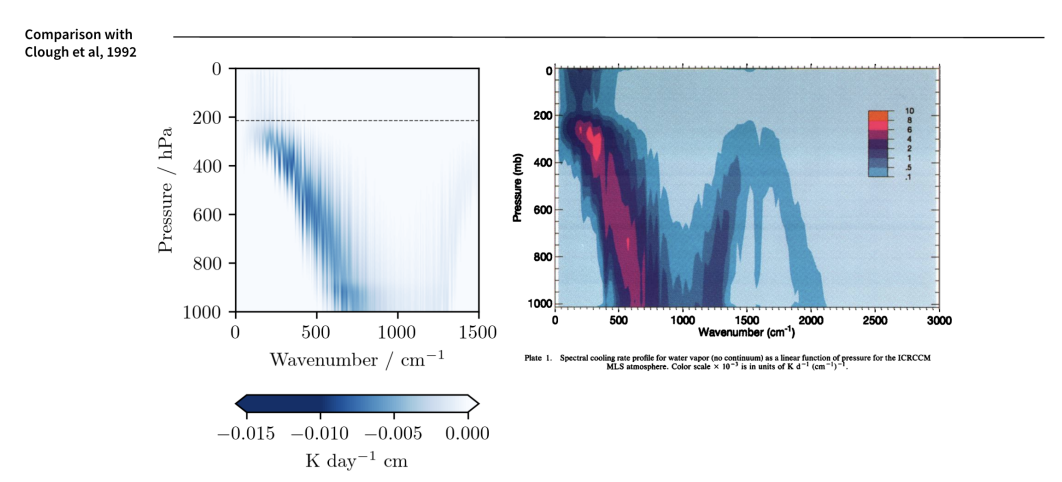


Figure S9. The correspondence between  $f_{\kappa}$  and the radiative tropopause are qualitatively similar for different values of stratospheric humidity. (First row) The amount of stratospheric water vapor passed to the offline radiation code is perturbed to a constant value. (Second row) The density of wavenumbers emitting to space at a given height,  $f_{\kappa}(p)$  are plotted for simulations with different values of water vapor. For the theory presented in the manuscript to hold and to be able to ignore stratospheric humidity, the value at the tropopause  $f_{tp}$  should be much smaller than the maximum value in the upper February 7, 2025, 10:29am troposphere. (Third row) Water vapor optical depth. (Fourth row) Spectrally-resolved longwave radiative cooling to space from water vapor.



**Figure S10.** Comparison of the spectrally resolved cooling to space in our model compared to Clough et al., 1992. (Left) The water vapor longwave radiative cooling to space in the simulation with ozone (Figure S5g) compared to Plate 1 of Clough et al., 1992.

Table S1. Definition of symbols used. See main text for details on computing  $\kappa_{\text{max}}$ . See Jeevanjee and Fueglistaler (2020) for more details and derivations of many of these quantities.

Symbol	Type	Description	Value/Units
$\nu$	Variable	Wavenumber	${ m cm}^{-1}$
$ au_{ m H_2O}$	Variable	Optical depth of water vapor at a given wavenumber	_
$\kappa_{ m H_2O}$	Variable	Spectroscopic absorption of water vapor at a given wavenumber	$\rm m^2~kg^{-1}$
$ ho_{ m H_2O}$	Variable	Density of water vapor	${\rm kg}~{\rm m}^{-3}$
$p_{ m ref}$	Constant	Reference atmospheric pressure	500 hPa
$p_{ m em}$	Variable	Emission pressure at a given wavenumber	hPa
$T_{ m em}$	Variable	Emission temperature at a given wavenumber	K
$T^*$	Constant	Characteristic temperature of water vapor	$LR_d\Gamma/(gR_v)\approx 960~\mathrm{K}$
$T_{ m ref}$	Variable	Characteristic tropospheric temperature	260 K
$T_{ m tp}$	Variable	Tropopause temperature	K
$M_v^{ m ref}$	Constant	Characteristic column water vapor mass	$T_{\rm ref} p_v^{\infty}/(\Gamma L) \approx 6 \cdot 10^9 \text{ kg m}^{-2}$
$p_v^\infty$	Constant	Reference value for the saturation vapor pressure	$2.5\cdot 10^{11}~\mathrm{Pa}$
$\kappa_{ m max}$	Constant	February 7, 2025, 10:29am Maximum absorption of water vapor	$\approx 5500~\mathrm{m^2~kg^{-1}}$
OLR	Variable	Outgoing longwave radiation	$ m Wm^{-2}$